Check for updates

Received: 16 July 2021 | Revised: 21 September 2021 | Accepted: 19 October 2021

DOI: 10.1002/cnm.3541

BASIC RESEARCH

WILEY

A finite element model to predict the consequences of endolymphatic hydrops in the basilar membrane

Bruno Areias[1] | **Marco P. L. Parente**[1,2] | **Fernanda Gentil**[3] | **Cristina Caroça**[4,5] | **João Paço**[4,5] | **Renato M. Natal Jorge**[1,2]

[1]INEGI, Institute of Science and Innovation in Mechanical and Industrial Engineering, Porto, Portugal

[2]FEUP, Faculty of Engineering, University of Porto, Porto, Portugal

[3]Escola Superior de Saúde – Politécnico do Porto, Clínica ORL – Dr. Eurico de Almeida, WIDEX, Porto, Portugal

[4]Núcleo académico-clínico de otorrinolaringologia e cirurgia cervico-facial do Hospital CUF Tejo/NOVA Medical School, Universidade Nova de Lisboa, Lisbon, Portugal

[5]Comprehensive Health Research Centre, NOVA Medical School, Universidade Nova de Lisboa, Lisbon, Portugal

Correspondence
Bruno Areias, INEGI, Institute of Science and Innovation in Mechanical and Industrial Engineering, Porto, Portugal.
Email: bareias@fe.up.pt

Funding information
Portuguese Foundation of Science and Technology, Grant/Award Number: UIDB/50022/2020; Ministério da Ciência, Tecnologia e Ensino Superior – Fundação para a Ciência e a Tecnologia, Grant/Award Number: SFRH/BD/129397/2017

Abstract

Ménière's disease is an inner ear disorder, associated with episodes of vertigo, fluctuant hearing loss, tinnitus, and aural fullness. Ménière's disease is associated with endolymphatic hydrops. Clinical evidences show that this disease is often incapacitating, negatively affecting the patients' everyday life. The pathogenesis of Ménière's disease is still not fully understood and remains unclear. Previous numerical studies available in the literature related with endolymphatic hydrops, are very scarce. The present work applies the finite element method to investigate the consequences of endolymphatic hydrops in the normal hearing, associated with the Ménière's disease. The obtained results for the steady state dynamics analysis are in accordance with clinical evidences. The results show that the basilar membrane is not affected in the same intensity along its length and that the lower frequencies are more affected by the endolymphatic hydrops. From a clinical point of view, this work shows the relationship between the increasing of the endolymphatic pressure and the development of hearing loss.

KEYWORDS

basilar membrane, cochlea, endolymphatic hydrops, hearing, Ménière's disease

1 | INTRODUCTION

In 1861, the French physician Prosper Ménière described, for the first time, a series of symptoms present in patients, caused by the inner ear, which became known as the Ménière's disease.[1,2] Ménière's disease is defined by the presence of episodes of spinning vertigo, sensorineural hearing loss and tinnitus or aural fullness during the attacks. The presence of sensorineural hearing loss during an episode of vertigo has been a key factor for the accurate diagnosis, as stated by Baloh.[3] A characteristic associated with the Meniere's disease is the dilatation of the endolymphatic compartment of the inner ear caused by an increase in endolymph.[4] High percentage of endolymphatic hydrops in affected ears with definite Ménière's disease has been reported using magnetic resonance imaging.[5]

Evidence shows that systemic autoimmune diseases such as rheumatoid arthritis, ankylosing spondylitis, and systemic lupus erythematosus may underlie the pathology of Ménière's disease.[6] The disease is 3 to 8-fold higher in the

 © 2021 John Wiley & Sons Ltd.

patients with systemic autoimmune diseases than in the general population.[7] According to Belinchon et al.,[8] the profile of sensorineural hearing loss in patients with unilateral differs from the patients with bilateral hearing loss. When an age correction has been applied, low tone hearing loss was observed in unilateral Ménière's disease, and a pantonal hearing loss was found in bilateral cases.[8] This finding is relevant, as far as the pantonal profile may be a predictor of bilateral hearing loss. As mentioned by Hatzopoulos et al.,[9] in the initial phase of the disease, the tonal audiometry revels a unilateral sensorineural hearing loss, affecting just the low frequencies. Furthermore, patients with Ménière's disease are more likely to have migraine, which may represent an endophenotype of this disease, as stated by Gazquez et al.[7] Several genes have been described in single familial with the Ménière's disease including FAM136A, DTNA, PRKCB, SEMA3D, and DPT, thus suggesting genetic heterogeneity. In addition, Roman et al.,[10] found using the gene burden analysis an enrichment of rare missense variants in several unrelated patients with familial Ménière's disease in the OTOG gene. Genetic findings in Ménière's disease are still in an early stage, without a main validated gene, as mentioned by Gallego and Lopez.[11]

According to Olivetto et al.,[12] Ménière's disease often affects only one ear, but the cases of bilateral disease are not rare. There are no differences with respect to gender, as mentioned by Vassiliou et al.[13] In Finland, the prevalence of the disease is at least 43 per 100,000 population.[14] Another study held in southern Finland showed a peak prevalence of 1709 per 100,000 in elderly people, aged between 61 and 70 years.[15] Ménière's disease is more frequent in European descendant populations than in other populations such as Asiatic or Native American.[16] Many authors state that the Ménière's disease prevalence seems to increase with age and the onset of symptoms appears around the third and fourth decade of life.[13,15,17,18] The study of Havia et al.[15] showed a decrease in the prevalence of the Ménière's disease in the older age groups, justifying such occurrence by the fact that some individuals with Ménière's disease have been excluded from the study by their numerous other diseases and symptoms, such as brain ischemia.

According Classification Committee of the Barany Society in cooperation with several national and international organizations and AAO-HNS Equilibrium Committee, Ménière disease was recently classified in definitive diagnosis and probable diagnosis depending on clinical appearance.[19,20] The clinical course usually is progressive and fluctuates unpredictably, where treatment is a challenge. The diagnostic criteria for definitive Ménière disease are based on two or more spontaneous attacks of vertigo, each lasting 20 min to 12 h; audiometrically documented fluctuating low to mid-frequency sensorineural hearing loss in the affected ear on at least one occasion before, during, or after one of the episodes of vertigo; fluctuating aural symptoms (hearing loss, tinnitus, or fullness) in the affected ear. Probable Ménière disease may be diagnosed based an occurrence of at least two episodes of vertigo or dizziness lasting 20 min to 24 h; fluctuating aural symptoms (hearing loss, tinnitus, or fullness) in the affected ear; other causes excluded by other tests.[20]

There are three longitudinal channels within the cochlea, the scala vestibuli, the scala tympani and a distinct channel, the scala media (Figure 1). In a healthy person, the endolymphatic (scala media) and the perilymphatic

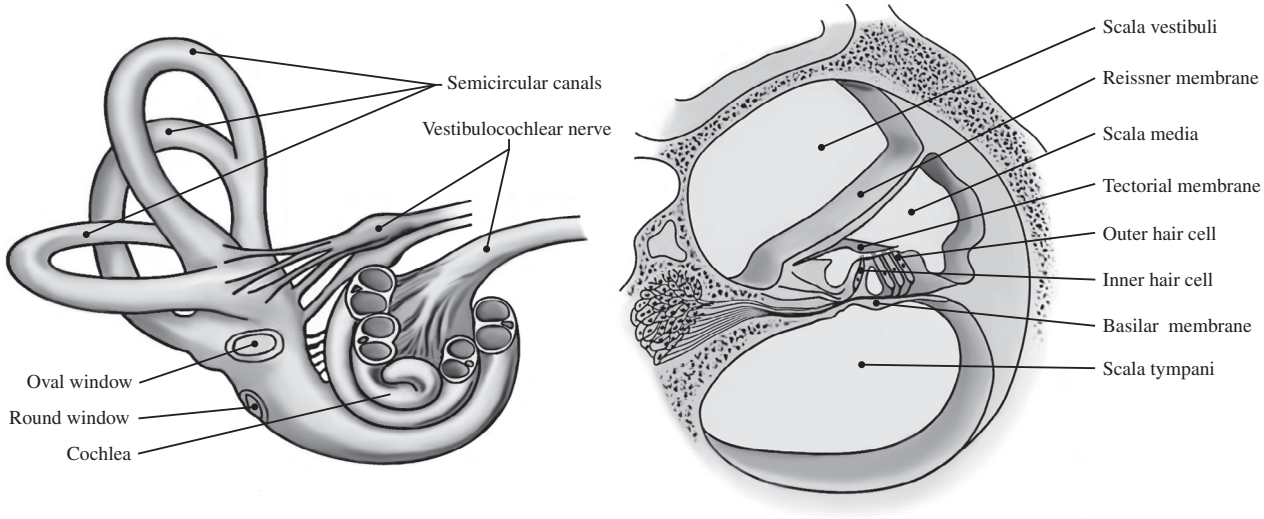

FIGURE 1 Anatomy of the human inner ear, adapted from *Neuroscience* by Purves[21]

20407947, 2022, 1, Downloaded from https://onlinelibrary.wiley.com/doi/10.1002/cnm.3541 by Estsp Politecnico Do Porto, Wiley Online Library on [22/02/2024]. See the Terms and Conditions (https://onlinelibrary.wiley.com/terms-and-conditions) on Wiley Online Library for rules of use; OA articles are governed by the applicable Creative Commons License

(scala vestibuli and tympani) pressure is equal and subjected to the same fluctuations.[22,23] Therefore, if the differential pressure between the endolymph and perilymph is different from zero, a deformation of the flexible structures, including the basilar membrane is expected.[24,25] This deformation tends to decrease the compliance of the basilar membrane, leading to a change in the natural frequency of its components and, in turn, the response of the auditory system.[4] In some cases, the differential pressure results in the rupture of the membrane. The presence of herniations and scarring due to prior ruptures as mentioned by Schuknecht and Gulya.[26] Rupture of the membrane may contribute to episodic vertigo symptoms and other functional changes in the inner ear.[27] Both electronystagmography and electrocochleography tests can be used to evaluate the presence of endolymphatic hydrops. Also, magnetic resonance assessment of the endolymphatic space using both IT and IV administration of GBCA can be performed, as mentioned by Conte et al.[28]

A large number of factors have been suggested as the cause for the development of endolymphatic hydrops. Paparella[29] and Merchant et al.[30] refer to causes such as the decreased endolymph absorption by the endolymphatic sac, the excessive endolymph production, genetic abnormalities, ionic imbalance (especially of sodium chloride), viral infections, autoimmune reactions, vascular irregularities, allergic responses, hypocellularity of the mastoid and penaqueductal air cells among others. As stated by Laine et al.,[31] saccular hydrops rarely appears with otosclerosis, although a possible cause of the hydrops is the obstruction of the vestibular aqueduct. For the majority of the patients, the current treatment of this disease includes drug therapies and lifestyle modifications. For rare cases, surgical treatments are applied. As stated by Haijin et al.,[32] drugs therapies are based in hydrochlorothiazide, potassium chloride sustained-release, and betahistine. Restrictions on consumption of salt, nicotine and alcohol intake are part of lifestyle modifications.

Therefore, in order to improve current treatments, it is important to understand the effects of the endolymphatic hydrops in the inner ear, more precisely in the basilar membrane. Using the finite element method, the present work intends to increase the knowledge of the endolymphatic hydrops and consequently the Ménière's disease and its influence on the basilar membrane. With the finite element method, it is possible to obtain a quantitative response on how the basilar membrane is affected along its length and what are the audible frequencies more affected by the endolymphatic hydrops.

2 | MATERIALS AND METHODS

The human cochlea has an intricate spiral shape (Figure 2). This anatomical geometry was considered on our work. It was obtained from a set of MRI images of a male patient, without cochlear pathologies. The width and thickness of the basilar membrane were acquired in the literature and assumed to change linearly from 100 μm at the base to 500 μm at the apex, and from 7.5 μm to 2.5 μm along the longitudinal direction, respectively.[33,34] The basilar membrane was considered with 31 mm in length.

The basilar membrane was divided along its length into equal parts. The length of each part was considered approximately 1 mm (see Figure 3). The shell elements (S4) used in the basilar membrane mesh have a characteristic length of .05 mm which provides a good accuracy. The division in parts enabled to impose the gradient of stiffness along the basilar membrane length, which is responsible for the frequency-place map of the cochlea, known as cochlear map. The scala media, the Reissner's membrane and the tectorial membrane were not considered in our work. The helicotrema allows the communication between the scala vestibuli and tympani, see Figure 3. As the cochlear map follows an exponential evolution,[35] it was then assumed, based on the work of Emadi et al.[36] that the mechanical properties should also vary in an exponential way. Thus, two exponential equations (Equations (1) and (2)) were formulated in order to describe the evolution of the Young's modulus, E_y, and the Rayleigh damping coefficient, β, along the basilar membrane. Both equations were determined through a calibration process, using with a sequence of numerical simulations in order to approximate the cochlear map obtained to the function proposed by Greenwood.[35]

$$\beta\,(\mathrm{s}) = 2 \times 10^{-6} e^{0.14x} \quad 0 < x < 31 \text{ mm} \tag{1}$$

$$E_y\,(\mathrm{MPa}) = -2.3e^{\frac{x}{12.2}} + 32 \quad 0 < x < 31 \text{ mm} \tag{2}$$

In contrast to the Equations (1) and (2), the Equations (3) and (4) use the distance, x_p, expressed as a proportion of the basilar membrane length from the round window, ranging between 0 and 1.

20407947, 2022, 1, Downloaded from https://onlinelibrary.wiley.com/doi/10.1002/cnm.3541 by Estsp Politecnico Do Porto, Wiley Online Library on [22/02/2024]. See the Terms and Conditions (https://onlinelibrary.wiley.com/terms-and-conditions) on Wiley Online Library for rules of use; OA articles are governed by the applicable Creative Commons License

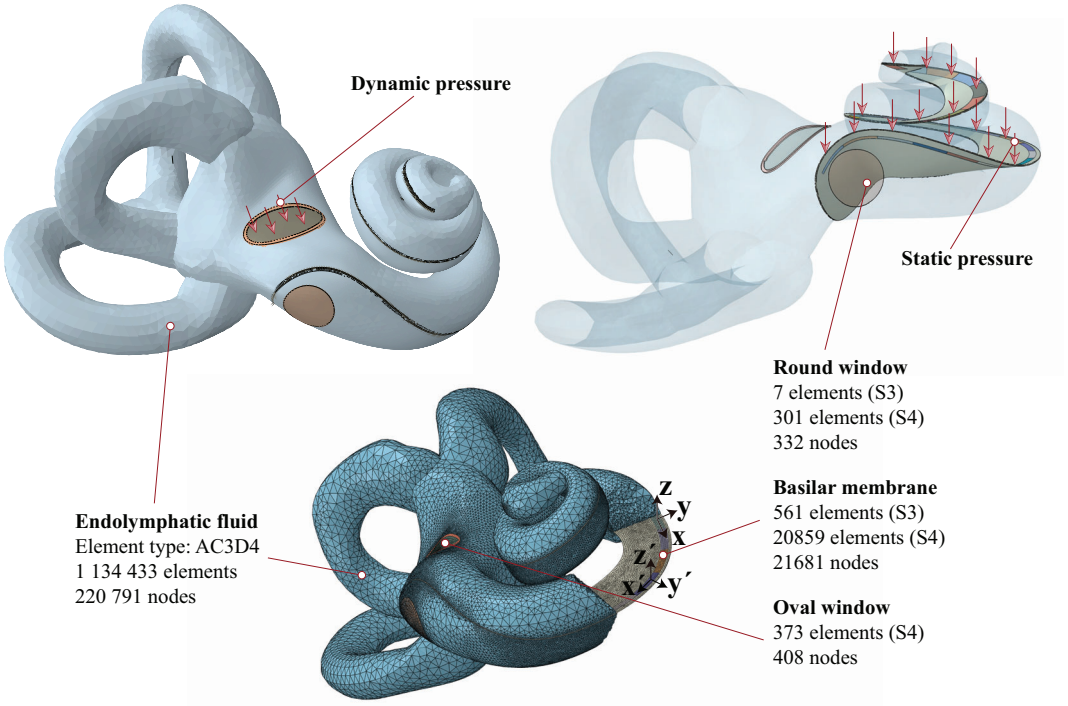

FIGURE 2 3D finite model of the inner ear. Red arrows show the location and direction of the static and dynamic pressure. Finite element mesh characterization of all parts

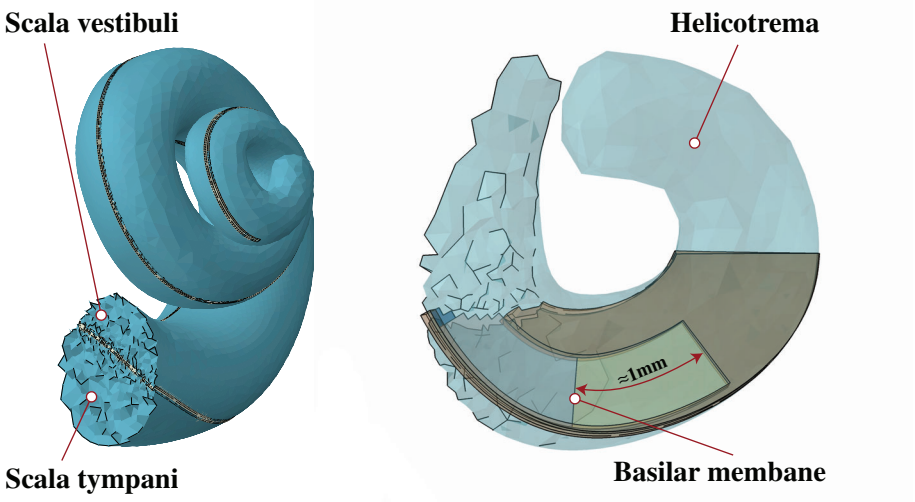

FIGURE 3 3D finite model of the inner ear. Detail of the scala vestibuli, the scala tympani, and the helicotrema

$$\beta\,(\mathrm{s}) = 2 \times 10^{-6} e^{4.34 x_p} \quad 0 < x_p < 1 \tag{3}$$

$$E_y\,(\mathrm{MPa}) = -2.3 e^{2.54 x_p} + 32 \quad 0 < x_p < 1 \tag{4}$$

The basilar membrane was modeled under plane stress conditions with shell elements. The Young's modulus in the transverse direction of the basilar membrane (direction of the radial fibers[37,38]) was defined by Equation (2). The distance, x, represents the distance from the base of the cochlea to the point of interest on the basilar membrane, expressed in mm. The longitudinal Young's modulus, E_x, expressed in MPa is then obtained through the equation $10E_x = E_y$. The basilar membrane was modeled with orthotropic properties, for which the following relations can be established,

20407947, 2022, 1, Downloaded from https://onlinelibrary.wiley.com/doi/10.1002/cnm.3541 by Estsp Politecnico Do Porto, Wiley Online Library on [22/02/2024]. See the Terms and Conditions (https://onlinelibrary.wiley.com/terms-and-conditions) on Wiley Online Library for rules of use; OA articles are governed by the applicable Creative Commons License

$$G_{xy} = G_{yz} \tag{5}$$

$$G_{xz} = \frac{E_x}{2(1+\nu_{xz})} \tag{6}$$

The shear modulus, G_{xy}, is related with E_y using Equation (7).[39,40]

$$G_{xy} = \frac{E_y}{2} \tag{7}$$

The Poisson's ratio was assumed after a series of iterations as $\nu_{xy} = \nu_{yz} = 0.2$ and $\nu_{xz} = 0.3$ in order to comply with the material stability requirements and also to achieve a cochlear map comparable to the Greenwood function. The density of the basilar membrane was considered to be $1200\,\mathrm{kg\,m^{-3}}$ and constant along its length. The perilymph was simulated considering water properties ($K = 2200\,\mathrm{MPa}$, $\rho = 1000\,\mathrm{kg\,m^{-3}}$ and inviscid). The Young's modulus, the Poisson's ratio and the density of the oval window and round window are summarized in the Table 1. As boundary conditions, the free edges of the oval window, the round window and the basilar membrane were considered fixed in all degree of freedom. The surfaces of the acoustic elements which contact the endosteum were considered as stationary rigid walls. The constructed 3D model was simplified, with only the passive mechanism being considered.

The 3D finite element model is composed by 243,212 nodes and 1,156,534 elements. Acoustic elements were used to model the perilymph. A dynamic load of .2 Pa (80 dB SPL) was applied to the stapes footplate in all numerical simulations (see Figure 2). The frequency band between 100 Hz and 10 kHz was considered in this study. The static pressure (see Figure 2) which allows to simulate the endolymphatic hydrops at two different stages was set at 67 Pa and 130 Pa. This pressure differential between both scalae were replaced by a mechanic pressure applied at the basilar membrane on the scala vestibuli side. A nonlinear static analysis was carried out at the first step to apply the static pressure. This step is followed by a steady state dynamic analysis that provides the steady state amplitude and phase of the response due to harmonic excitation at a given frequency. Both analysis were carried out using the commercial software Abaqus Standard.[45]

In a linear elastic material behavior, the total stress, $\boldsymbol{\sigma}$, is related to the total elastic strain, $\varepsilon^{\mathrm{el}}$, through the elasticity tensor, D^{el}, as follows.

$$\boldsymbol{\sigma} = D^{\mathrm{el}}\varepsilon^{\mathrm{el}} \tag{8}$$

In order to define an orthotropic material subdivided with shell elements under plane stress conditions, only the values E_x, E_y, ν_{xy}, G_{xy}, G_{xz}, and G_{yz} are needed. The shear moduli G_{xz} and G_{yz} are listed because may be required for modeling the transverse shear deformation in a shell. Thus, the elasticity tensor can be defined by the Equation (9).

$$D^{\mathrm{el}} = \begin{bmatrix} \frac{1}{E_x} & -\frac{\nu_{xy}}{E_x} & 0 \\ -\frac{\nu_{xy}}{E_x} & \frac{1}{E_y} & 0 \\ 0 & 0 & \frac{1}{G_{xy}} \end{bmatrix} \tag{9}$$

TABLE 1 Mechanical properties of the inner ear parts (Young's modulus, Poisson's ratio, and density)

	Inner ear parts	E (MPa)	ν (—)	ρ ($\mathrm{kg\,m^{-3}}$)
Oval window	Stapes footplate[41–43]	14,100	.3	2500
	Stapedial annular ligament[41,44]	.6		1200
	Round window[33]	.35		1200

20407947, 2022, 1, Downloaded from https://onlinelibrary.wiley.com/doi/10.1002/cnm.3541 by Estsp Politecnico Do Porto, Wiley Online Library on [22/02/2024]. See the Terms and Conditions (https://onlinelibrary.wiley.com/terms-and-conditions) on Wiley Online Library for rules of use; OA articles are governed by the applicable Creative Commons License

In an acoustic medium, the constitutive behavior of the fluid is assumed to be inviscid and compressible, so that, the dynamic pressure, p, relates to the volumetric strain, ε_v, through the bulk modulus, K_f, as expressed by the Equation (10).

$$p = -K_f \varepsilon_v \tag{10}$$

3 | RESULTS

Figure 4 shows the magnitude and phase of the basilar membrane velocity relative to stapes footplate velocity at 12 mm from the round window. The numerical results obtained were compared with experimental data reported in the literature in order to validate the model. The experimental results reported by Stenfelt et al.[46] which were acquired from a human cadaver temporal bone at 12 mm from the round window are represented in Figure 4. The data of Gundersen et al.[47] extracted using the Mössbauer technique and recalculated later by Stenfelt et al.[46] was also included. The resonance peak is very similar between the compared data. The response of Stenfelt et al.[46] and Gundersen et al.[47] resonate at approximately 2 kHz and 3.6 kHz, respectively. Our findings showed a resonance peak near 2.5 kHz that is in accordance with the experimental data. The phase angle has the same tendency of the experimental results. The sharp decrease of the phase angle above 3 kHz suggests the presence of the traveling wave inside the cochlea. An increase in the basilar membrane velocity relative to stapes footplate is observed between 7 kHz and 9 kHz.

Figure 5 shows the cochlear map obtained using the finite element model of the passive normal cochlea and the respective comparison with the function proposed by Greenwood[35] and the experimental results published by Békésy in 1960.[48] In this work, the active mechanism present in the outer hair cell, which provides a local positive feedback along the cochlear partition, as mentioned by Ren and Gillespie,[49] was not considered. The cochlear map correlates the location of maximum vibration of the basilar membrane as a function of frequency along the basilar membrane, this frequency is termed characteristic frequency. The results obtained are close to the data obtained in the literature, which allowed to validate the model. In Figure 5 the cochlear map for different pressures applied on the basilar membrane is also shown, thus simulating the endolymphatic hydrops at two different stages. The curve "FE model normal" shows the response of the basilar membrane in normal condition or when it is not under any static pressure. For lower frequencies, which are captured at locations near the apex of the cochlea, major changes were found, as the static pressure increased. Such differences are also shown in the Figure 6 in terms of magnitude of the basilar membrane displacement. No notorious differences at higher frequencies were registered, as can be seen in Figures 5 and 6. The basilar membrane changed the mode of vibration mainly at lower frequencies. There was no notorious peak of displacement near the apex when the static pressure differential was applied, as expected for a normal traveling wave developed

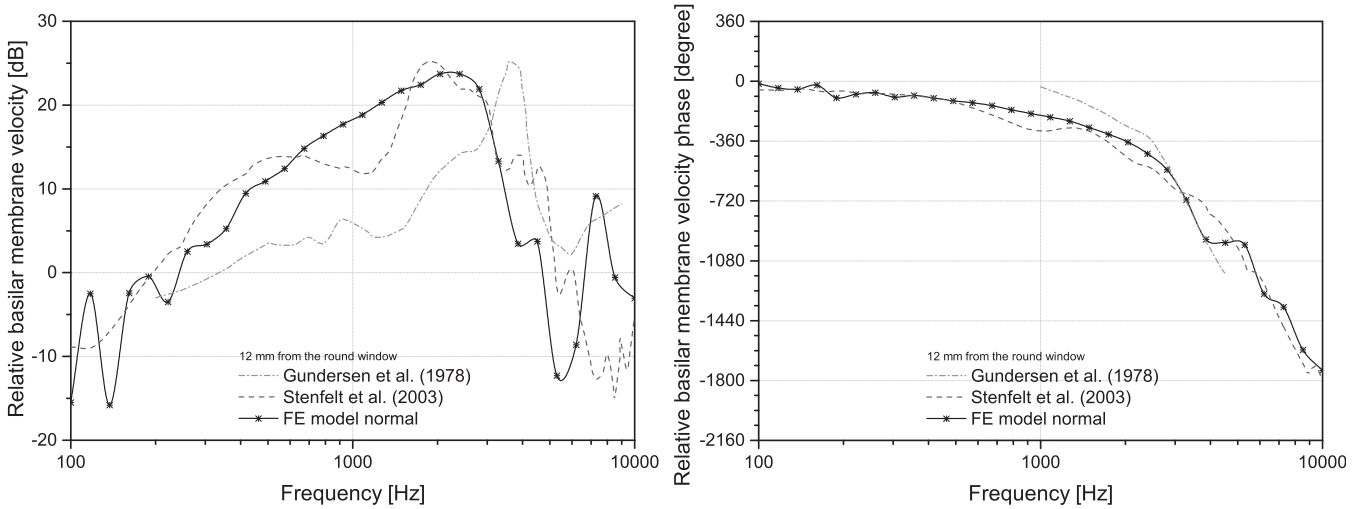

FIGURE 4 Comparison and validation of the magnitude and phase of basilar membrane velocity relative to stapes footplate velocity with experimental results at 12 mm from the round window

20407947, 2022, 1, Downloaded from https://onlinelibrary.wiley.com/doi/10.1002/cnm.3541 by Estsp Politecnico Do Porto, Wiley Online Library on [22/02/2024]. See the Terms and Conditions (https://onlinelibrary.wiley.com/terms-and-conditions) on Wiley Online Library for rules of use; OA articles are governed by the applicable Creative Commons License

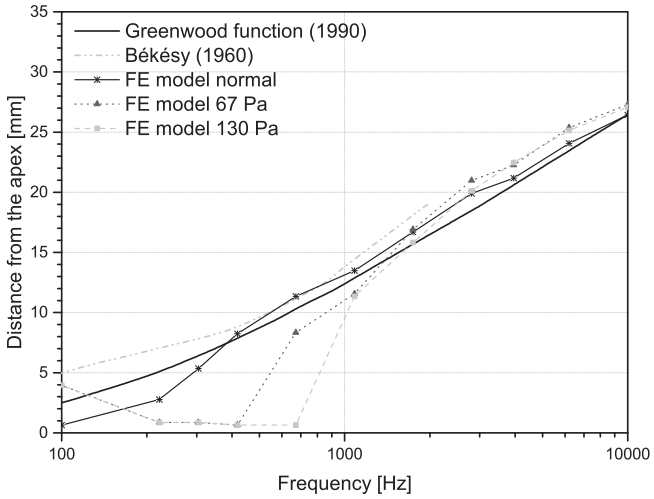

FIGURE 5 Cochlear map validation and comparison with different endolymphatic hydrops stages

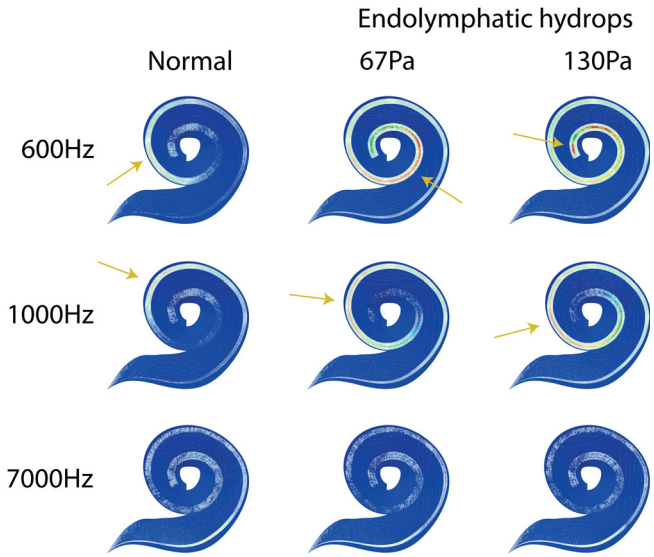

FIGURE 6 Magnitude of the basilar membrane displacement at 600 Hz, 1000 Hz, and 7000 Hz for normal condition and two endolymphatic hydrops stages

inside the cochlea (see Figure 6). The peak of displacement was also less pronounced and extended to lower frequencies as the static pressure increased. In summary, the increase in static pressure reduced the frequency selectivity present in a normal cochlea.

Figure 7 shows the magnitude and the phase of the displacement in the basilar membrane at 19 from the apex of the cochlea. The maximum value of the displacement did not change when the static pressure differential was applied, neither did the frequency nor the amplitude. The phase of the displacement shows a sharp decrease at the same frequency, for which the maximum displacement was observed, thus showing the presence of the traveling wave. In short, the application of a static pressure differential had reduced effects in the response of the basilar membrane at positions near the base of the cochlea, where the higher frequencies are captured.

Figure 8 shows the magnitude and phase of the basilar membrane near the middle of the basilar membrane, more precisely, at 15 mm from the apex of the cochlea. At this location, the basilar membrane shows to be highly affected by the static pressure. There is a decrease in the magnitude and an increase in the frequency at which the maximum displacement was obtained, as the static pressure increased. A decrease of 6 dB and 9 dB in the magnitude of the displacement was recorded due to a static pressure of 67 Pa and 130 Pa, respectively. The phase of the displacement indicated to be affected by static pressure. As expected, the sharp decrease of the phase was registered at a higher frequency, as

20407947, 2022, 1, Downloaded from https://onlinelibrary.wiley.com/doi/10.1002/cnm.3541 by Estsp Politecnico Do Porto, Wiley Online Library on [22/02/2024]. See the Terms and Conditions (https://onlinelibrary.wiley.com/terms-and-conditions) on Wiley Online Library for rules of use; OA articles are governed by the applicable Creative Commons License

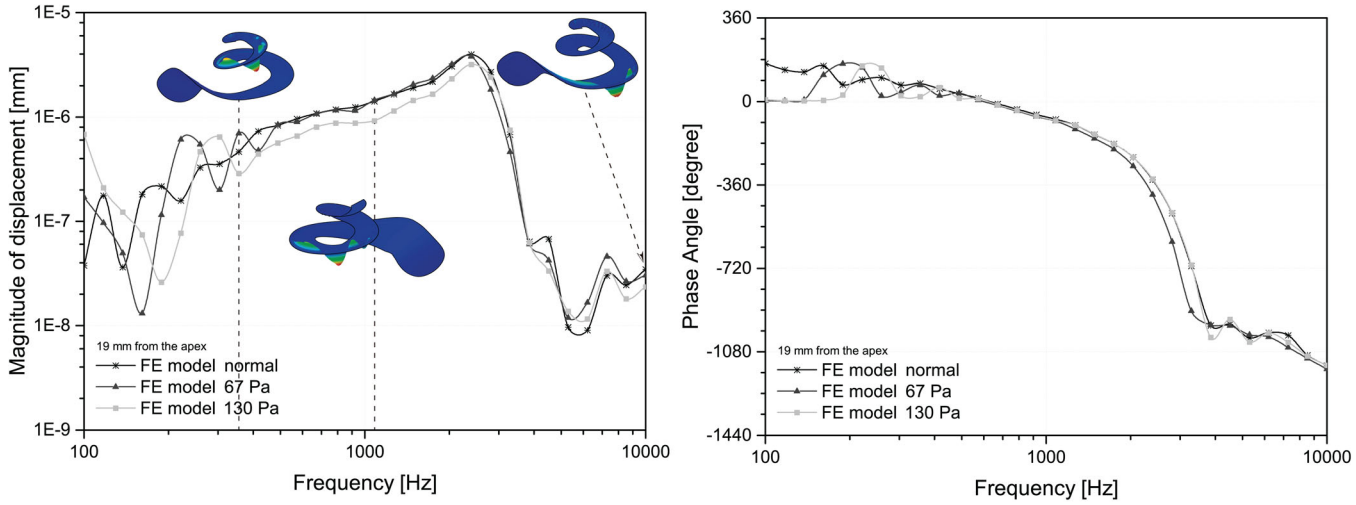

FIGURE 7 Magnitude and phase of the basilar membrane displacement at 19 mm from the apex of the cochlea. Basilar membrane illustrations correspond to the FE model normal, the displacement was amplified

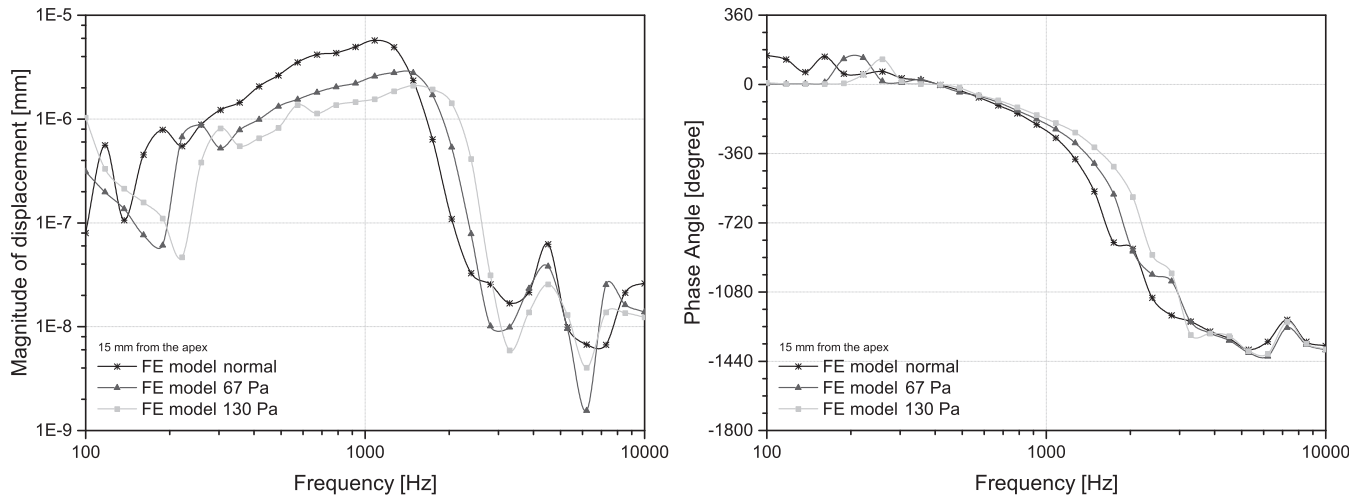

FIGURE 8 Magnitude and phase of the basilar membrane displacement at 15 mm from the apex of the cochlea

the static pressure increased. Such changes in the dynamic behavior of the basilar membrane can be explained by the increase of the basilar membrane stiffness owing to the static pressure applied.[50]

Figure 9 shows the response of the basilar membrane at 7 mm from the apex of the cochlea. At this location, the obtained results showed that the basilar membrane is highly affected. The tendency is the same as the previous position, near the middle of the cochlea, but more pronounced. A decrease in the magnitude of 12 dB and 16 dB was recorded for 67 Pa and 130 Pa pressure differentials, respectively. There was also a considerable change in the phase, increasing the frequency at which the sharp decrease was observed.

In order to study the influence of the static pressure on the maximum displacement of the basilar membrane, a static pressure between 0 Pa and 130 Pa was applied. Figure 10 shows the evolution of the maximum displacement in the basilar membrane for different static pressures inside the mentioned range. The maximum displacement is always located at the apex of the cochlea (where the basilar membrane stiffness is lower; see illustration in Figure 10) and follows approximately a logarithmic evolution. Therefore, a logarithmic fit was also included in Figure 10. The static pressure of 130 Pa is not enough to deform the basilar membrane and touch the bottom of the scala tympani.

20407947, 2022, 1, Downloaded from https://onlinelibrary.wiley.com/doi/10.1002/cnm.3541 by Estsp Politecnico Do Porto, Wiley Online Library on [22/02/2024]. See the Terms and Conditions (https://onlinelibrary.wiley.com/terms-and-conditions) on Wiley Online Library for rules of use; OA articles are governed by the applicable Creative Commons License

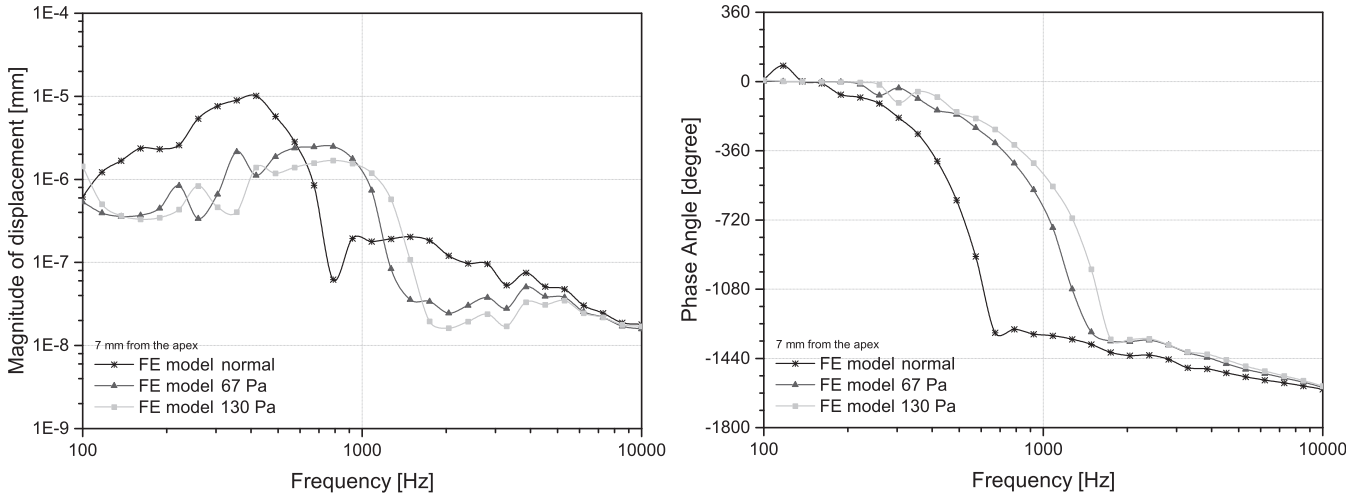

FIGURE 9 Magnitude and phase of the basilar membrane displacement at 7 mm from the apex of the cochlea

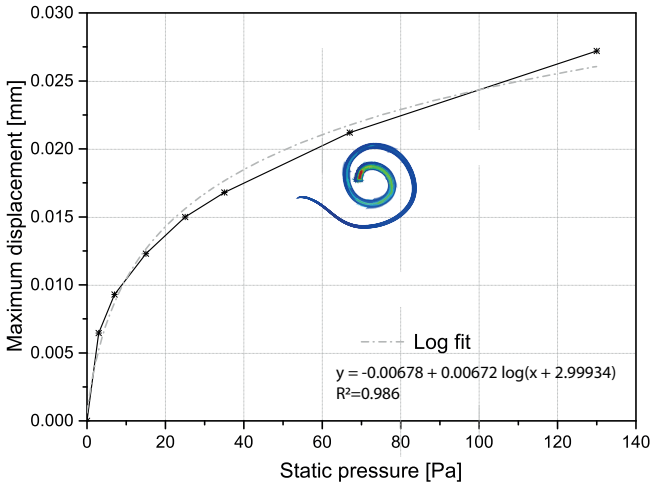

FIGURE 10 Maximum displacement of the basilar membrane imposed by the static pressure

4 | DISCUSSION

Unlike already published works in literature, the present study applies an exponential approach to the mechanical properties of the basilar membrane and employs a cochlear spiral shape based on magnetic resonance images. Most of the works in the literature, by contrast, simplify the geometry of the cochlea, considering it as a tapered box. Since our work is based in MRI, such irregular geometry can lead to the presence of peaks as observed between 7 kHz and 9 kHz. However, the peak observed is smaller than half of the maximum registered, which result in a lesser importance.

Among the limitations of the present study, our model does not incorporate the Reissner membrane nor the tectorial membrane. However, both membranes can explain the transient hearing loss in early stages, once these membranes need a lower pressure to be deformed in comparison with the basilar membrane. Thus, a study of the Reissner membrane and tectorial membrane should be developed in future works with some modifications on the finite element model.

The early stage of chronic hydrops occurs with minimal change in pressure (<67 Pa) between endolymph and perilymph. The pressure value was based in the experimental work of Böhmer which used guinea pigs in his study. The usage of experimental models, mainly guinea pigs and rats have the advantage of being easy to handle, and their ears are very similar to those of humans, as mentioned by Albuquerque et al.[51] At this stage, the negligible increase of the pressure is mainly due to the high flexibility of the endolymphatic boundaries which allows the endolymph volume to grow without a high increase in the pressure.[27,52] It is known that high differences of pressure between the endolymph

20407947, 2022, 1, Downloaded from https://onlinelibrary.wiley.com/doi/10.1002/cnm.3541 by Estsp Politecnico Do Porto, Wiley Online Library on [22/02/2024]. See the Terms and Conditions (https://onlinelibrary.wiley.com/terms-and-conditions) on Wiley Online Library for rules of use; OA articles are governed by the applicable Creative Commons License

and the perilymph affects the resonant characteristics of the basilar membrane. In the study of Böhmer,[53] a pressure gradient of approximately 125 Pa, corresponding to a pressure gradient 100 times higher than the one caused by the sound pressure of loud tones, was able to strongly affect the normal behavior of the basilar membrane. Accordingly, for the severe endolymphatic hydrops a pressure differential of 130 Pa was considered on the present work.[54] The degree of the endolymphatic hydrops can be associated with the decrease in the basilar membrane displacement.

Three different points along the basilar membrane were used to extract the numerical results. These points were selected with the intention of capturing the influence of the endolymphatic hydrops at the low, medium, and high frequencies, which are the three frequency bands frequently used in clinical environment.

The endolymphatic hydrops can result in an increase of the basilar membrane displacement at some frequencies as shown in Figures 7–9. However, the position where is identified the maximum amplitude of displacement (near the characteristic frequency) tends to decrease its amplitude which will result in deficient stimulation of the vestibulocochlear nerve and consequently a reduction of hearing. Accordingly, it is important to study the location around the maximum amplitude where the vibration will be translated into hearing. The results obtained on this study, using the finite element method are in agreement with the experimental results available in the literature, which describes the lower frequencies as the first frequency band to be affected, due to the influence of the endolymphatic hydrops on the basilar membrane response.[55–57] Tinnitus, a perception of noise or ringing sounds is common in people with the Ménière's disease. In almost all the cases of tinnitus, the perceived tones are confined to low tones or low pitch tones.[18,58] The symptoms appear to be linked with the apex of the cochlea and to be a consequence of the static pressure present inside the scala media.

Diplacusis, a pathology where patients, for a given pure single-frequency stimulus, perceive two different frequency sounds (one frequency from each ear) may also be a consequence of the endolymphatic hydrops. The basilar membrane frequency shift can explain this pathology because a single frequency sound can be perceived as a slightly lower frequency.

5 | CONCLUSIONS

Ménière's disease is a disorder of the inner ear that is characterized by a set of unpleasant and painful symptoms. The cause of Ménière's disease is still unclear but likely involves both genetic and environmental factors. This disease affects the dynamic behavior of the basilar membrane, but not equally along its length, thus representing a higher hearing loss at specific audible frequencies. Using the finite element method, it is possible to investigate the consequences and the changes that the endolymphatic hydrops causes in the inner ear and hearing. This work shows the relationship between the increasing of the endolymphatic pressure and the development of hearing loss. Therefore, a steady state dynamic analysis was conducted in the audible frequency range, between 100 Hz and 10 kHz. Two static pressures, 67 Pa and 130 Pa differentials were applied to the basilar membrane, thus simulating the endolymphatic hydrops. Our finite element model shows that the endolymphatic hydrops affects mainly the lower frequencies. As expected, the static pressure leads to greater deformations near the apex of the cochlea, where the stiffness is lower. Such deformation follows approximately a logarithmic evolution, and, in this context a logarithmic fit was formulated. Thus, from a biomedical point of view it is then expected that the hearing loss should be more accentuated on the lower frequencies. For these frequencies, a high pitched sound becomes heard as low pitched (see Figure 6), if the basilar membrane amplitude is able to trigger the mechanotransduction process, since the peak of the traveling wave changes its frequency to a location nearest to the apex. Based on the numerical analysis, patients with endolymphatic hydrops are not expected to develop complications on higher frequencies. From our numerical study, we can see that with the increasing static pressure, the basilar membrane is increasingly affected toward the round window. Since the portion of the basilar membrane closer to the round window presents a higher stiffness, it will be less affected by a small change in the static pressure, when compared to the region closer to the apex of the cochlea, where the stiffness is lower. In addition, the static pressure can theoretically affect the motion of the hair cells, mainly decoupling them from the tectorial membrane. In such cases, if the disease is left untreated, it is known that the hearing loss will reach the remaining frequencies, and may even result in a permanent hearing loss. Accordingly, diplacusis may be a consequence of the endolymphatic hydrops. The basilar membrane frequency shift can explain the diplacusis because a single frequency sound can be perceived as a slightly lower frequency so patients with endolymphatic hydrops can perceive two different frequency sounds corresponding to a given single-frequency sound. Tinnitus, a symptom of the Ménière's disease, arises mainly at low-pitch sounds, probably indicating deafness on these frequencies. Other diseases, such as otosclerosis,

20407947, 2022, 1, Downloaded from https://onlinelibrary.wiley.com/doi/10.1002/cnm.3541 by Estsp Politecnico Do Porto, Wiley Online Library on [22/02/2024]. See the Terms and Conditions (https://onlinelibrary.wiley.com/terms-and-conditions) on Wiley Online Library for rules of use; OA articles are governed by the applicable Creative Commons License

occurs with hearing loss at low frequencies. Nonetheless, endolymphatic hydrops presents other symptoms, for example, vertigo or balance problems that otosclerosis does not. Such differences will help to distinguish different pathologies with hearing loss at low frequencies.

In the present work, a more realistic distribution of the pressure and propagation of the traveling wave was obtained due to the usage of a non-linear function to describe the basilar membrane properties and an improved geometrical description of the cochlear shape.

The outcomes obtained in this work, intend to support the medical community to ensure a swift detection of the disease, based on the symptoms described by the patients, such as a poor hearing at low frequencies, thus resulting in a rapid and efficient treatment, avoiding its spread to values that may result in permanent hearing loss.

ACKNOWLEDGMENTS

The authors truly acknowledge the funding provided by Ministério da Ciência, Tecnologia e Ensino Superior – Fundação para a Ciência e a Tecnologia (Portugal), under grant: SFRH/BD/129397/2017. This research was also supported by the Portuguese Foundation of Science and Technology under the research project UIDB/50022/2020.

CONFLICT OF INTEREST

The authors declare that there is no financial, professional or other personal interest of any nature or kind in any product, service and/or company that could be constructed as influencing the position.

DATA AVAILABILITY STATEMENT

Data sharing not applicable to this article as no datasets were generated or analysed during the current study.

ORCID

Bruno Areias https://orcid.org/0000-0001-9583-3571
Renato M. Natal Jorge https://orcid.org/0000-0002-7281-579X

REFERENCES

1. Ménière P. Mémoire sur des lésions de l'oreille interne donnant lieu à des symptômes de congestion cérébrale apoplectiforme. *Gazette médicale de Paris*. 1861;16:597-601.
2. Ménière P. Sur une forme de sourdité grave dépendant d'une lésion de l'oreille interne. *Gazette médicale de Paris*. 1861;16:29.
3. Baloh RW. Prosper Meniere and his disease. *Arch Neurol*. 2001;58(7):1151-1156.
4. Hallpike CS, Cairns H. Observations on the pathology of Meniere's syndrome. *Proc R Soc Med*. 1938;31(11):1317-1336.
5. Okazaki Y, Yoshida T, Sugimoto S, et al. Significance of endolymphatic hydrops in ears with unilateral sensorineural hearing loss. *Otol Neurotol*. 2017;38(8):1076-1080.
6. Kim SH, Kim JY, Lee HJ, Gi M, Kim BG, Choi JY. Autoimmunity as a candidate for the etiopathogenesis of Meniere's disease: detection of autoimmune reactions and diagnostic biomarker candidate. *PLoS One*. 2014;9(10):e111039.
7. Gazquez I, Soto-Varela A, Aran I, et al. High prevalence of systemic autoimmune diseases in patients with Meniere's disease. *PLoS One*. 2011;6(10):e26759.
8. Belinchon A, Perez-Garrigues H, Tenias JM, Lopez A. Hearing assessment in Meniere's disease. *Laryngoscope*. 2011;121(3):622-626.
9. Hatzopoulos S, Ciorba A, Corazzi V, Skarzynski PH. OAEs and Meniere disease. In: Jr FB, ed. *Up to Date on Meniere's Disease*. IntechOpen; 2017.
10. Roman-Naranjo P, Gallego-Martinez A, Soto-Varela A, et al. Burden of rare variants in the OTOG gene in familial Meniere's disease. *Ear Hear*. 2020;41(6):1598-1605.
11. Gallego-Martinez A, Lopez-Escamez JA. Genetic architecture of Meniere's disease. *Hear Res*. 2020;397:107872.
12. Olivetto E, Simoni E, Guaran V, Astolfi L, Martini A. Morphological and functional structure of the inner ear: its relation to Ménière's disease. *Audiol Med*. 2012;10(4):160-166.
13. Vassiliou A, Vlastarakos PV, Maragoudakis P, Candiloros D, Nikolopoulos TP. Meniere's disease: still a mystery disease with difficult differential diagnosis. *Ann Indian Acad Neurol*. 2011;14(1):12-18.
14. Kotimaki J, Sorri M, Aantaa E, Nuutinen J. Prevalence of Meniere disease in Finland. *Laryngoscope*. 1999;109(5):748-753.
15. Havia M, Kentala E, Pyykko I. Prevalence of Meniere's disease in general population of southern Finland. *Otolaryngol—Head Neck Surg*. 2005;133(5):762-768.
16. Perez-Carpena P, Lopez-Escamez JA. Current understanding and clinical management of Meniere's disease: a systematic review. *Semin Neurol*. 2020;40(1):138-150.
17. Celestino D, Ralli G. Incidence of Meniere's disease in Italy. *Am J Otol*. 1991;12(2):135-138.
18. Caparosa RJ. Medical treatment for Meniere's disease. *Laryngoscope*. 1963;73:666-672.

20407947, 2022, 1, Downloaded from https://onlinelibrary.wiley.com/doi/10.1002/cnm.3541 by Estsp Politecnico Do Porto, Wiley Online Library on [22/02/2024]. See the Terms and Conditions (https://onlinelibrary.wiley.com/terms-and-conditions) on Wiley Online Library for rules of use; OA articles are governed by the applicable Creative Commons License

19. Committee on hearing and equilibrium guidelines for the diagnosis and evaluation of therapy in Menière's disease. American Academy of Otolaryngology-Head and Neck Foundation, Inc. *Otolaryngol Head Neck Surg*. 1995;113(3):181-185.
20. Lopez-Escamez JA, Carey J, Chung WH, et al. Diagnostic criteria for Menière's disease. *J Vestib Res*. 2015;25(1):1-7.
21. Purves D. *Neuroscience*. 6th ed. Oxford University Press; 2018.
22. Nomura Y. *Morphological Aspects of Inner Ear Disease*. 1st ed. Springer Japan; 2014.
23. Takeuchi S, Takeda T, Saito H. Pressure relationship between perilymph and Endolymph associated with endolymphatic infusion. *Ann Otol Rhinol Laryngol*. 1991;100(3):244-248.
24. Mucha A, Fedor S, DeMarco D. Vestibular dysfunction and concussion. *Handb Clin Neurol*. 2018;158:135-144.
25. Charpiot A, Fath L, Veillon F, Venkatasamy A, Baumgartner D. The dynamics of endolymphatic hydrops and vestibular disorders. *J Vestib Res*. 2021;31(4):247-249.
26. Schuknecht HF, Gulya AJ. Endolymphatic Hydrops—an overview and classification. *Ann Otol Rhinol Laryngol*. 1983;92(5):1-20.
27. Salt AN, Plontke SK. Endolymphatic hydrops: pathophysiology and experimental models. *Otolaryngol Clin North Am*. 2010;43(5): 971-983.
28. Conte G, Lo Russo FM, Calloni SF, et al. MR imaging of endolymphatic hydrops in Méniére's disease: not all that glitters is gold. *Acta otorhinolaryngologica Italica: organo uffciale della Societa italiana di otorinolaringologia e chirurgia cervico-facciale*. 2018;38(4):369-376.
29. Paparella MM. Pathogenesis of Meniere's disease and Meniere's syndrome. *Acta Otolaryngol Suppl*. 1984;406:10-25.
30. Merchant SN, Adams JC, Nadol JBJ. Pathophysiology of Meniere's syndrome: are symptoms caused by endolymphatic hydrops? *Otol Neurotol*. 2005;26(1):74-81.
31. Laine J, Hautefort C, Attye A, et al. MRI evaluation of the endolymphatic space in otosclerosis and correlation with clinical findings. *Diagn Interv Imaging*. 2020;101(9):537-545.
32. Haijin Y, Hong G, Chunhong W, Yin X. Management of Meneere's disease—the Beijing Tiantan hospital experience. *J Otol*. 2014;9(2): 106-109.
33. Gan RZ, Reeves BP, Wang X. Modeling of sound transmission from ear canal to cochlea. *Ann Biomed Eng*. 2007;35(12):2180-2195.
34. Liu W, Atturo F, Aldaya R, et al. Macromolecular organization and fine structure of the human basilar membrane - RELEVANCE for cochlear implantation. *Cell Tissue Res*. 2015;360(2):245-262.
35. Greenwood DD. A cochlear frequency-position function for several species - 29 years later. *J Acoust Soc Am*. 1990;87(6):2592-2605.
36. Emadi G, Richter CP, Dallos P. Stiffness of the gerbil basilar membrane: radial and longitudinal variations. *J Neurophysiol*. 2004;91(1): 474-488.
37. Iurato S. Functional implications of the nature and submicroscopic structure of the tectorial and basilar membranes. *J Acoust Soc Am*. 1962;34:1386-1395.
38. Teudt IU, Richter CP. Basilar membrane and tectorial membrane stiffness in the CBA/CaJ mouse. *J Assoc Res Otolaryngol*. 2014;15(5): 675-694.
39. Kim Y, Kim JS, Kim GW. A novel frequency selectivity approach based on travelling wave propagation in mechanoluminescence basilar membrane for artificial cochlea. *Sci Rep*. 2018;8:12023.
40. Ren L, Cheng H, Ding GH, Yang L, Dai PD, Zhang TY. Three-dimensional finite element hydrodynamical modeling of straight and spiral cochlea. *AIP Conf Proc*. 2018;1965(1):030003.
41. Areias B, Santos C, Jorge RN, Gentil F, Parente MP. Finite element modelling of sound transmission from outer to inner ear. *Proc Inst Mech Eng Pt H, J Eng Med*. 2016;230(11):999-1007.
42. Sun Q, Gan RZ, Chang KH, Dormer KJ. Computer-integrated finite element modeling of human middle ear. *Biomech Model Mechanobiol*. 2002;1(2):109-122.
43. Gentil F, Parente MP, Martins P, et al. The inuence of the mechanical behaviour of the middle ear ligaments: a finite element analysis. *Proc Inst Mech Eng Pt H, J Eng Med*. 2011;225(1):68-76.
44. Gan RZ, Yang F, Zhang X, Nakmali D. Mechanical properties of stapedial annular ligament. *Med Eng Phys*. 2011;33(3):330-339.
45. Dassault Systemes. *ABAQUS Analysis User's Guide*; Dassault Systèmes Simulia Corp; 2016.
46. Stenfelt S, Puria S, Hato N, Goode RL. Basilar membrane and osseous spiral lamina motion in human cadavers with air and bone conduction stimuli. *Hear Res*. 2003;181(1–2):131-143.
47. Gundersen T, Skarstein O, Sikkeland T. A study of the vibration of the basilar membrane in human temporal bone preparations by the use of the Mossbauer effect. *Acta Otolaryngol*. 1978;86(3–4):225-232.
48. Von Békésy G. *Experiments in Hearing*. McGraw-Hill; 1960.
49. Ren T, Gillespie PG. A mechanism for active hearing. *Curr Opin Neurobiol*. 2007;17(4):498-503.
50. Lee S, Koike T. Simulation of the basilar membrane vibration of endolymphatic hydrops. *Procedia IUTAM*. 2017;24:64-71.
51. Albuquerque AAS, Rossato M, de Oliveira JAA, Hyppolito MA. Understanding the anatomy of ears from Guinea pigs and rats and its use in basic otologic research. *Braz J Otorhinolaryngol*. 2009;75(1):43-49.
52. Long CH, Morizono T. Hydrostatic pressure measurements of endolymph and perilymph in a Guinea pig model of endolymphatic hydrops. *Otolaryngol Head Neck Surg*. 1987;96(1):83-95.
53. Böhmer A. Hydrostatic pressure in the inner ear uid compartments and its effects on inner ear function. *Acta Otolaryngol Suppl*. 1993; 507:3-24.
54. Böhmer A. Experimental endolymphatic hydrops and inner ear pressure. In: Ernst A, Marchbanks R, Samii M, eds. *Intracranial and Intralabyrinthine Fluids*. Springer; 1996:81-84.

20407947, 2022, 1, Downloaded from https://onlinelibrary.wiley.com/doi/10.1002/cnm.3541 by Estsp Politecnico Do Porto, Wiley Online Library on [22/02/2024]. See the Terms and Conditions (https://onlinelibrary.wiley.com/terms-and-conditions) on Wiley Online Library for rules of use; OA articles are governed by the applicable Creative Commons License

55. Ding CR, Xu XD, Wang XW, et al. Effect of Endolymphatic Hydrops on sound transmission in live Guinea pigs measured with a laser Doppler vibrometer. *Neural Plast*. 2016;2016:8648297.
56. Brown CS, Emmett SD, Robler SK, Tucci DL. Global hearing loss prevention. *Otolaryngol Clin North Am*. 2018;51(3):575-592.
57. Magnan J, Ozgirgin ON, Trabalzini F, et al. European position statement on diagnosis, and treatment of Meniere's disease. *J Int Adv Otol*. 2018;14(2):317-321.
58. Douek E, Reid J. The diagnostic value of tinnitus pitch. *J Laryngol Otol*. 1968;82(11):1039-1042.

How to cite this article: Areias B, Parente MPL, Gentil F, Caroça C, Paço J, Natal Jorge RM. A finite element model to predict the consequences of endolymphatic hydrops in the basilar membrane. *Int J Numer Meth Biomed Engng*. 2022;38(1):e3541. doi:10.1002/cnm.3541

20407947, 2022, 1, Downloaded from https://onlinelibrary.wiley.com/doi/10.1002/cnm.3541 by Estsp Politecnico Do Porto, Wiley Online Library on [22/02/2024]. See the Terms and Conditions (https://onlinelibrary.wiley.com/terms-and-conditions) on Wiley Online Library for rules of use; OA articles are governed by the applicable Creative Commons License